Large urban parks summertime cool and wet island intensity and its influencing factors in Beijing, China

Yilun Li [a,b,c], Shuxin Fan [a,b], Kun Li [a,b], Yue Zhang [a,b], Lingxu Kong [a,b], Yafen Xie [a,b], Li Dong [a,b,*]

[a] School of Landscape Architecture, Beijing Forestry University, Beijing, 100083, China
[b] Beijing Laboratory of Urban and Rural Ecological Environment, Beijing, 100083, China
[c] AECOM, Beijing, 100025, China

ARTICLE INFO

ABSTRACT

Construction of urban parks has long been proved as an effective way to mitigate urban heat island effect, and better arrangement of green spaces in a city is expected to help regulate urban climate. To provide further empirical evidence and guidance for urban green spaces planning and design, field measurement of summertime air temperature and relative humidity was conducted in and out of 10 large urban parks in Beijing, China. Averaged daytime and nighttime park cool and wet island intensity were 1.09 ℃, 1.48 % and 3.63 ℃, 4.25 % respectively. Parks' influence on local-scale climate extended as far as over 1km during summer nights, and more effective cooling effects were provided within approximately one-park width. Among all influencing factors, park size plays dominant role in regulating nighttime local-scale climate in parks' adjacent area, while vegetation coverage around sampling points out of urban parks also has significant contributions, indicating that large urban parks and their surrounding urban greenery interact to affect neighborhood climate. Park size was the only factor found correlated with nocturnal park cool and wet island intensity. Results of this study provide additional information on large urban parks' local-scale climate effect and give insights to future urban green spaces planning and design practice.

1. Introduction

Compared to pre-industrial period, the world is estimated to have become warmer by 0.8–1.2 ℃ (Allen et al., 2018). Besides this global warming trend, urban heat island effect, a phenomenon featuring higher temperature in a city than in its surrounding rural area (Oke, 1995), brings more challenges to city dwellers. Man-made constructions change the thermal properties of underlying surfaces, while human activities release a large quantity of anthropogenic heat (Oke et al., 2017), which largely deteriorates summertime thermal environment. Urban expansion is projected to induce a 0.5−0.7 ℃ on average and up to ˜3 ℃ summertime air temperature (Ta) increase by 2050 (Huang et al., 2019). Finding ways to mitigate adverse effects of continuous warming in cities, especially in summer when considering fatal heat stress (Kovats and Hajat, 2008), is of great importance.

Urban parks, composed mainly of vegetation and water bodies, not only are cool islands in cities, but also can influence their adjacent areas (Bartesaghi Koc et al., 2018; Bowler et al., 2010; Taleghani, 2018).

Thermal properties of vegetation and water body differentiate the thermal environment in a park from its surrounding area. Vegetation cools the air mainly through shading and evapotranspiration (Taha et al., 1991). And water bodies, featuring high heat capacity, reduce increase of Ta during daytime, while serve as heat source at night (Oke, 1992). It is through convection that cool air in parks gets transferred to their vicinity area, and therefore influences the local-scale climate (Sugawara et al., 2021).

Field measured Ta and remotely sensed land surface temperature (LST) are widely used for the assessment of park cool island intensity (PCII) and its influencing factors. Multiple spatial parameters, including park size (PS), park's shape, land cover configuration and adjacent land use had been investigated mostly by using LST (Masoudi and Tan, 2019; Xu et al., 2017; Yang et al., 2017), largely due to its easy access to simultaneously collected data of a large area. While research implementing field measurement is also of great significance for its close relationship with thermal comfort and perception (Epstein and Moran, 2006). However, most studies implementing Ta measurement focus on

---

the cooling effect of one or few individual parks (e.g., Barradas, 1991; Shashua-Bar and Hoffman, 2000; Cohen et al., 2012; Doick et al., 2014; Yan et al., 2018), and there are still limited studies that compared atmospheric PCII among multiple urban parks at one time (Chang and Li, 2014; Chang et al., 2007; Jaganmohan et al., 2016; Monteiro et al., 2016). Chang et al. (2007) and Jaganmohan et al. (2016) studied atmospheric PCII of 61 and 62 urban parks in Taipei, China and Leipzig, Germany respectively, which are the studies that involved the most urban parks in quantity. Besides, Monteiro et al. (2016) compared atmospheric PCII among 8 parks in London, Britain. These studies mainly focused on small parks in a city, with medians of PS as 0.6, 2.2 and 2.7 ha.

PS, a key parameter that is highly relevant to urban green spaces planning and design, has been paid the most attention in park cooling effect studies. Some studies have identified the smallest PS that could guarantee a stable cooling effect (Chang et al., 2007; Monteiro et al., 2016), and have observed a non-linear relation between PS and PCII (Chang et al., 2007; Yu et al., 2020b). A threshold perspective, which refers to the decrease of park cooling efficiency when exceeds certain PS, was brought up as a reference for finding best green spaces layout (Yu et al., 2017). Previous studies all indicate local thresholds smaller than or around 10 ha (Yang et al., 2020; Yu et al., 2017; Chang et al., 2007; Monteiro et al., 2016). Although such theory seems to imply that scattered small parks in a city can better regulate urban climate than one large park, large urban parks are necessities in a city for their indispensable ecological and recreational functions. Works done by Jauregui (1990); Doick et al. (2014) and Yan et al. (2018) are not yet enough to depict the local-scale climate effect of large urban parks in cities.

Beijing, the capital city of China, has undergone rapid urbanization in the past decades, and its thermal environment has deteriorated in the last tens of years (Peng et al., 2016). The frequent urban renewal and new constructions of urban green spaces serve as opportunities to improve its thermal environment. Providing additional knowledge on parks' cool and wet island effects, especially local ones when considering that park's cooling effect is possibly climate-sensitive (Bowler et al., 2010; Saaroni et al., 2018), may serve as references for future planning and design practice.

Therefore, we conducted field measurement of Ta and relative humidity (Rh) in and around 10 large urban parks in Beijing, China to find answers to the following questions: (1) How strong are PCII and park wet island intensity (PWII) of urban parks in Beijing, China? (2) How strong does large urban parks influence local climate around the parks? (3) What are the influencing factors on large urban parks' local-scale climate effects?

2. Methodology

2.1. Study sites

Beijing (39°56′N, 116°20′E) is the capital city of China, located in the northwest of North China Plain, and has a total area of 16410 km². It features a warm temperate semi humid continental monsoon influenced climate. In 2019, the precipitation was 406.3 mm; the annual average air temperature was 13.8℃; and the average air temperatures of July and August were 28.0℃ and 25.9℃ respectively (NBSC, 2020).

Ten urban parks located within the 4th Ring Road of Beijing were selected as study sites, whose sizes range 15.21–285.25 ha. Their basic information and abbreviations are listed in Table 1 and their locations are shown in Fig. 1. According to the information on the website of Beijing Municipal Administration Center of Parks, there are over 50 urban parks located within the 4th Ring Road, whose sizes range from less than 1–285.25 ha. The ten parks we selected are among the large ones in central Beijing. Liuyin Park, the smallest park selected in this research, is the 24th largest park within 4th Ring Road in Beijing.

Table 1
Study sites and their basic information.

Study site	PS (ha)	PerV	PerW	PerI
Liuyin Park (LYP)	15.21	0.59	0.31	0.10
Qingnianhu Park (QNHP)	18.07	0.59	0.22	0.19
Jingshan Park (JSP)	25.15	0.72	0	0.28
Ditan Park (DTP)	36.76	0.72	0	0.28
Zizhuyuan Park (ZZYP)	45.23	0.57	0.31	0.12
Taoranting Park (TRTP)	52.32	0.60	0.26	0.14
Beihai Park (BHP)	68.52	0.31	0.54	0.15
Yuyuantan Park (YYTP)	126.06	0.42	0.45	0.13
Tiantan Park (TTP)	198.03	0.74	0	0.26
Chaoyang Park (CYP)	285.25	0.55	0.17	0.28

PS Park size, *PerV* Percentage of vegetation coverage, *PerW* Percentage of water coverage, *PerI* Percentage of impervious surfaces.

2.2. Measurement of air temperature and relative humidity

Ta and Rh were measured at the height of 1.2 m with Fluke 971 Temperature Humidity Meter. The accuracy of the device is ±0.5 ℃ and ±2.5 %, and the resolution is 0.1 ℃ and 0.1 %, meeting the requirements of ISO 7726 (ISO, 1998). This device also features short reaction time of less than 60 s. The external Ta and Rh sensors of the device is surrounded by its porous black shield which may both provide protection and partly avoid direct exposure to sunshine. And to further avoid the influence of direct sun exposure, we used an umbrella with black ultraviolet protection coating approximately 1 m above the device during data collection. Measurements were taken on clear days with gentle winds that had similar weather conditions in July and August 2019, which is the hottest time of the year in Beijing. Sampling dates and the background meteorology conditions were listed in Appendix A. Sampling times were at noon starting at around 13:00, and at night starting at around 20:30. Each sampling process was less than 80 min. Past research on urban green spaces' thermal effects has focused on multiple time periods, e.g., at noon (Li et al., 2021; Jiao et al., 2017), in the afternoon (Lin et al., 2017; Yan et al., 2018; Jiao et al., 2017), at night (Lin et al., 2017; Yan et al., 2018; Li et al., 2021; Dorigon and Amorim, 2019), at midnight (Coseo and Larsen, 2014), before dawn (Altunkasa and Uslu, 2020; Sodoudi et al., 2018), etc. Due to the different thermal properties of built areas and vegetation, urban heat island intensity peaks several hours after sunset (Oke et al., 2017; Doick et al., 2014). However, because of the park administration policy that all selected parks in this research are closed between 21:00 to 06:00, nighttime data sampling were arranged as late as possible to obtain a PCII value close to the peak value.

Fig. 1 shows the location of all sampling and reference points. In each park, three nonshaded sampling points which are around 100 m apart and located close to the park geometric center were selected. One north-south orientation road adjacent to the park was selected as sampling routes, on which numerous nonshaded sampling points were selected. These points were mainly located near road intersections or on squares to avoid shadings from trees or buildings. The length of the sampling route was approximately one to two park-width away from the park but no more than 2 km, for locations at one park-width was frequently used as reference point in previous research (Chang and Li, 2014; Jaganmohan et al., 2016), while the cooling extent of the largest park in Beijing is no more than 2 km (Yan et al., 2018). Data collection in and around ZZYP, TRTP, YYTP, TTP and CYP was conducted independently. Data collection in and around JSP and BHP was conducted in one sampling process, for these two parks are relatively close, and so it was for LYP, QNHP and DTP. At each sampling point, three Ta and Rh were measured with a 30 s interval after the device had stabilized and averaged for data analyses. UniStrong UG908 GPS Terminal was used to record geographic information.

Considering that the measurements at each point were not simultaneous, one nonshaded reference point was chosen on a public square
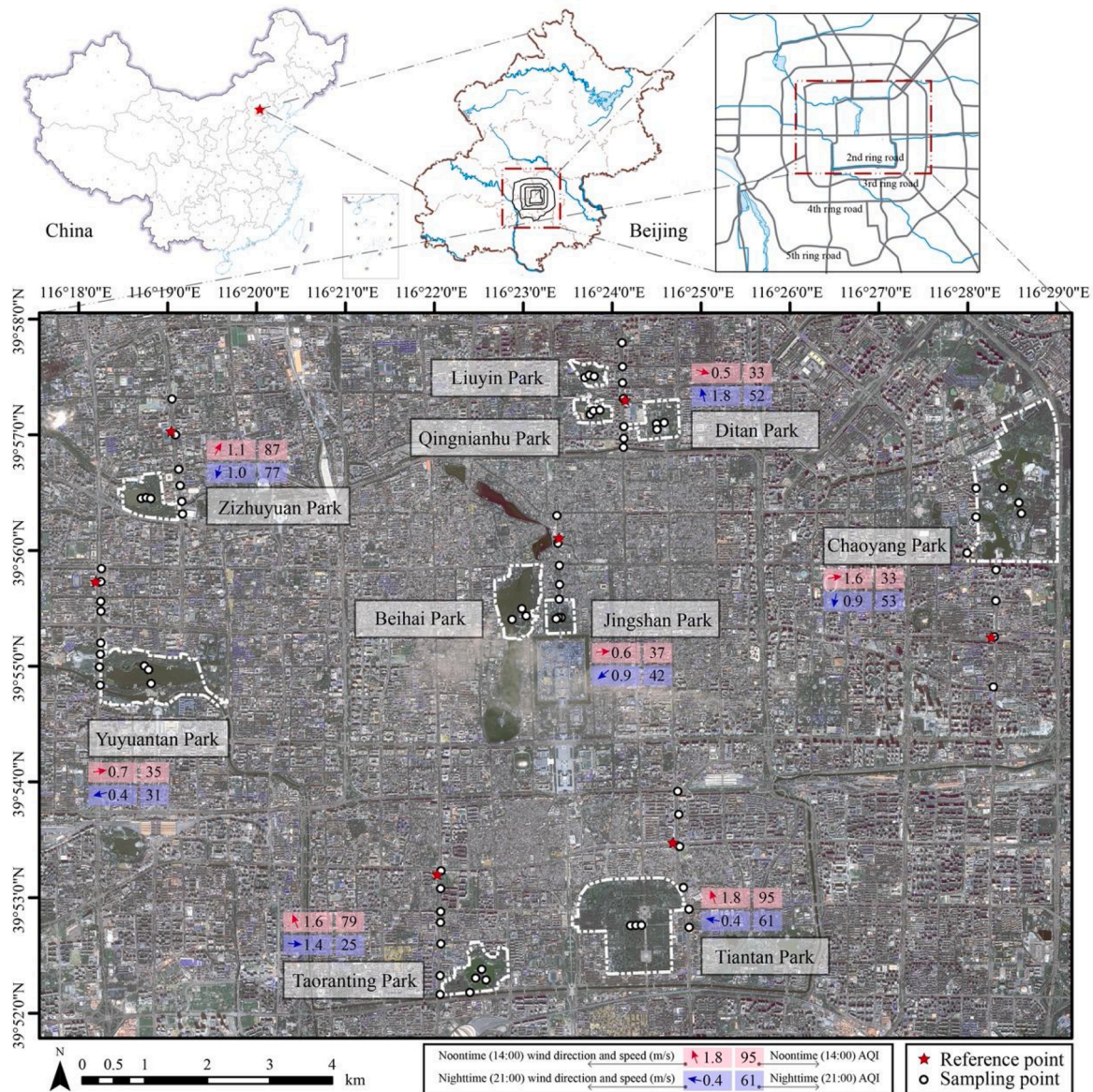
Fig. 1. Locations of study sites and sampling points (Wind direction, wind speed and AQI (air quality index) data were collected from local meteorology and air quality monitoring station. For detailed background meteorology data and data source, see Appendix A.).

along the sampling route, and four Ta and Rh were recorded with 30 s interval for every 10 min by using another Fluke 971 Temperature Humidity Meter. Local Ta and Rh were presumed to have changed linearly, whose change rates were calculated using average Ta and Rh of every 10 min at the reference point. And the change rates were further used for the calibration of collected data along the route.

2.3. Measurement of influencing factors

We investigated the influence of land cover composition, the shape of urban parks and the spatial location of sampling points on Ta and Rh.

GF-2 image with four multi-spectral bands (4 m resolution) and 1 panchromatic band (0.8 m resolution) acquired on August 31 and September 5, 2018 were used for land cover classification. We combined supervised classification and visual interpretation to identify three land cover types in each urban park and around each sampling point, namely vegetation, water body and impervious surfaces. Supervised classification of vegetation and non-vegetation was conducted in ENVI 5.3 using maximum likelihood method, while park boundaries and water bodies within study area were visually interpreted. Land cover maps of the

three land cover types were further produced by subtracting visually interpreted water body area from non-vegetation area in ArcGIS 10.2. The percentage of each land cover type in each individual park is calculated, as shown in Table 1. In addition, for all sampling points out of urban parks, the percentage of each land cover type within 50 m and 100 m radius buffer zone is calculated. Previous studies carried out in urban canyons in Beijing indicates that land cover composition within approximately 100 m radius has prominent influence on urban climate (Yan et al., 2014a, 2014b).

Landscape shape index (LSI) of each urban park was calculated following the formula below:

$$LSI = \frac{0.25E}{\sqrt{A}}$$

Where E represents the perimeter of an urban park (m), while A represents the area of the urban park (m^2).

The distance from the sampling point around ZZYP, TRTP, YYTP, TTP and CYP to the geometric center of each park (DTC) was calculated in ArcGIS 10.2. Moreover, relative distance (RD) was further calculated
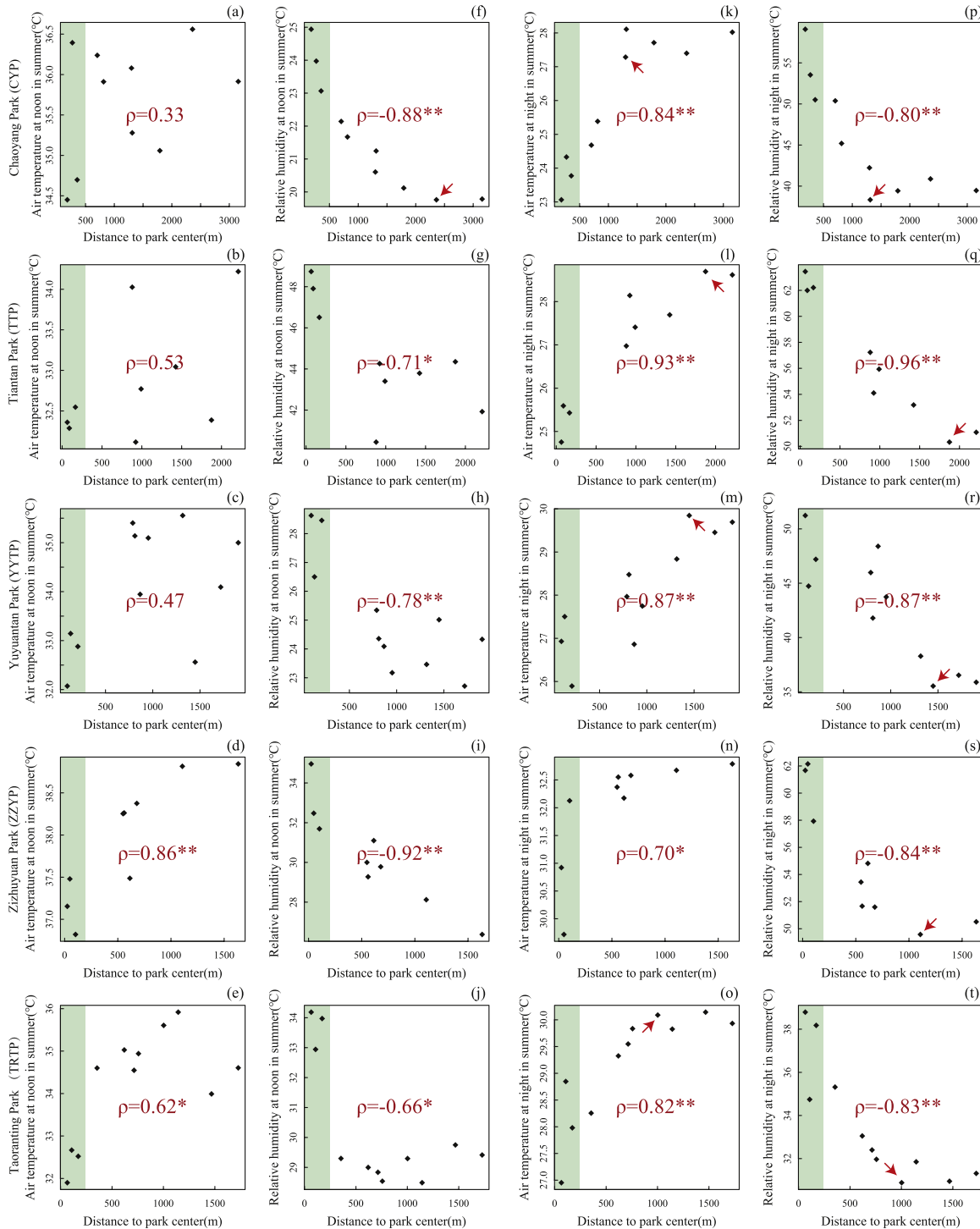
following the formula below:

$$RD = \frac{D_{ij}}{\sqrt{A_i}}$$

Where D_{ij} represents the distance from sample j around park i to park j's geometric center (m), while A_i represents the area of the urban park (m^2). This factor is designed to evaluate parks' climate effect on their surrounding area based on their size.

2.4. Data analyses

For data collected in and around ZZYP, TRTP, YYTP, TTP and CYP, t-test was performed to compare Ta and Rh in and out of each urban park. The scatter plots of Ta, Rh and the distance from the sampling points to the park geometric center were drawn, and their Pearson correlations were calculated using R package Hmisc (Harrell, 2018).

In addition, dTa and dRh were calculated following the formulas below:

Fig. 2. Scatter plots and Pearson correlations between Ta, Rh and the distance from sampling points to park geometric center (Points with green shading are samples located within parks. Red arrows point at the point that could be visually identified as the turning point.). (For interpretation of the references to colour in this figure legend, the reader is referred to the web version of this article).

$$dTa_{ij} = Ta_{ij} - Ta_{ave_j}$$

$$dRh_{ij} = Rh_{ij} - Rh_{ave_j}$$

Where Ta_{ij} and Rh_{ij} refer to Ta and Rh of sampling point i out of urban park j, and Ta_{ave_j} and Rh_{ave_j} refer to average Ta and Rh of three sampling points within park j. Pearson correlations between dTa, dRh and the influencing factors, including PS, RD and the percentage of different land cover types around each sampling points out of the urban parks, were calculated. Linear and polynomial regression models were built when correlations detected. For non-linear regressions, we intentionally found the point whose derivative equals ± 1 as the turning point, which could be used as a representation of efficiency changes in parks cooling effects, as similarly defined by Fan et al. (2018). Additionally, multiple linear regressions were performed with correlated factors as independent variables to identify which factor contribute the most to dTa and dRh.

For data collected in and around DTP, LYP, QNHP, JSP and BHP, one-way ANOVA was performed to compare Ta and Rh in and out of urban parks. R package multcomp (Hothorn et al., 2008) was used to conduct Tukey multiple comparison at α = 0.05.

PCII of each urban park is calculated by subtracting the average Ta of three sampling points within the urban park from the average Ta of all sampling points out of the urban park, while PWII is calculated the opposite way. Thus, a positive PCII or PWII indicates a cool or wet island in city. Pearson correlations between PCII, PWII and influencing factors, including PS, LSI, PerV, PerW and PerI, were calculated. Linear regression models were built to estimate the trend between PCII, PWII and correlated factors.

All data analyses were conducted on R 3.5.3 (R Development Core Team, 2015). Graphics were depicted in R and further edited in Adobe Illustrator when needed.

3. Results

3.1. Park' influence on Ta and Rh gradients out of urban parks

Fig. 2 shows the scatter plots and Pearson correlations between Ta, Rh out of 5 parks and the distance from sampling points to park geometric center. Pearson correlation coefficients show that nighttime Ta and Rh in and out of urban parks are better linearly correlated with DTC than daytime, indicating more significant Ta and Rh gradients at night. Even though the limited quantity of data we collected around each park is insufficient to identify precise cooling or humidifying distances through building statistical models, certain trends are clearly demonstrated in the scatter plots. Ta out of urban parks gradually increases while Rh decreases as sampling points get further away from the park, and remains steady from a certain point. Some of the potential turning point could be visually identified by comparing it with its nearby points (Fig. 2(f), (k)–(m), (o)–(t)), as shown in Fig. 2 with the red arrows. Such trends are more obvious during nighttime, and parks' influence on their adjacent area could extend as far as over 1 km during summer nights

(Fig. 2(k)–(m), (o)–(t))

Table 2 shows the correlation coefficients between dTa, dRh of sampling points out of 5 urban parks and the influencing factors. Compared with daytime dTa and dRh, better correlations are detected at night. Larger parks are found to have better cooling and humidifying effects at night in summer (Table 2, ρ = 0.59**, ρ=-0.51**).

We further built regression models between nighttime dTa, dRh and correlated factors, as shown in Fig. 3. Regression models demonstrate that DTC has better linear relationship with dTa and dRh than RD (Fig. 3 (a)–(d)), featuring higher R^2. Better regression models are established between dTa, dRh and RD non-linearly (Fig. 3(e) and (f)) than linearly (Fig. 3(c) and (d)), with higher R^2. As the sampling points get further away from parks, dTa gradually increases, while its increasing speed decreases (Fig. 3(e)). While dRh complies with the opposite trend (Fig. 3 (f)). By calculating the point at which the derivative equals ± 1, more effective cooling and humidifying effects of parks at night in summer extend as far as 0.978 and 1.874 times of park width respectively.

The land cover composition around each sampling points out of urban parks also have a significant influence on nighttime dTa and dRh. Higher vegetation and water coverage may lead to lower dTa and higher dRh at night (Fig. 3(g) and (h)), indicating a significant cooling and humidifying effect of urban greening and water bodies on the neighborhood, which counteracts the local-scale climate effects of the large urban parks.

We further used multiple linear regression models to distinguish the dominant influencing factor by comparing the standardized coefficients among different correlated factors. Considering that the 5 parks are different in size, RD rather than DTC was chosen as an independent variable to quantify the importance of different factors. Significant regression models were built for nighttime dTa and dRh when PS, RD and PerV$_{100}$ were included, as shown in Table 3. Compared with RD and PerV$_{100}$, PS plays dominant role in influencing nighttime dTa and dRh (β = 0.64, β=-0.55), indicating that larger parks have stronger local climate effects. Coefficients of RD (β = 0.40, β=−0.37), a factor related to the spatial location of sampling points, indicate that the closer to parks, the stronger local climate effects exist. While PerV$_{100}$, mostly comprised of urban greenery such as street trees, pocket gardens, community gardens, etc., also play important roles in regulating local-scale climate in the area adjacent to parks.

3.2. Park cool and wet island intensity

Table 4 shows PCII and PWII of the 10 selected urban parks and Fig. 4 shows the comparison of Ta and Rh in and out of 10 urban parks. Stronger PCII and PWII (Table 4), and more significant Ta and Rh differences (Fig. 4) were observed during summer nighttime than daytime. All 10 parks were found cooler than their surrounding areas, with PCII ranging 0.11–2.54 ℃ at noon and 0.35–3.22 ℃ at night. These parks were also 1.64–4.69 % wetter than their surrounding areas during summer daytime, while not always wetter, ranging −5.79−12.11 %, at night.

Correlation coefficients between PCII, PWII and different park

Table 2
Correlation coefficients between influencing factors and dTa, dRh out of 5 urban parks.

	PS	DTC	RD	PerW		PerV		PerI	
				50 m	100 m	50 m	100 m	50 m	100 m
dTa at noon	**−0.54****	−0.19	0.20	0.13	0.23	0.20	0.30	−0.21	−0.32
dRh at noon	0.25	−0.21	−0.41*	−0.02	0.08	0.16	0.13	−0.15	−0.13
dTa at night	**0.59****	**0.77****	0.33	**−0.35***	**−0.39***	**−0.42***	**−0.57****	**0.47****	**0.59****
dRh at night	**−0.51****	**−0.69****	**−0.34***	0.30	**0.41***	**0.46****	**0.57****	**−0.50****	**−0.60****

dTa Difference of air temperature, ***dRh*** Difference of relative humidity, *PS* Park size, *DTC* Distance to park center, *RD* Relative distance, ***PerW*** Percentage of water coverage, ***PerV*** Percentage of vegetation coverage, ***PerI*** Percentage of impervious surfaces. Same below.

* p < 0.05 (two-tail).
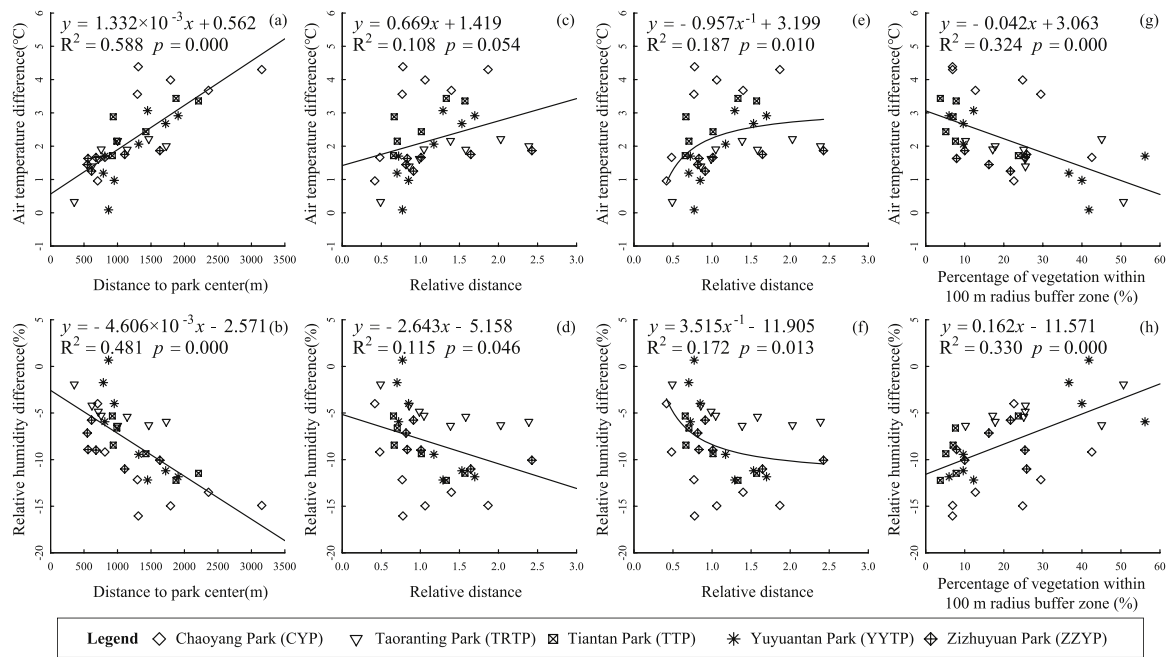** p < 0.01 (two-tail).

Fig. 3. Regression models of nighttime dTa, dRh and correlated influencing factors.

Table 3
Multiple regression models of dTa and dRh at night in summer.

	dTa at night			dRh at night		
	B	β	p	B	β	p
PS (ha)	7.42×10^{-3}	0.64	0.000 **	-2.41×10^{-2}	−0.55	0.000 **
RD	0.81	0.40	0.001 **	−2.89	−0.37	0.006 **
PerV$_{100}$ (%)	-2.45×10^{-2}	−0.33	0.004 **	1.02×10^{-1}	0.36	0.006 **
Interception	0.74	–	0.120	−3.66	–	0.080
R^2	0.70			0.61		
Adjusted R^2	0.67			0.57		
p	0.000**			0.000**		

B coefficient, **β** standardized coefficient, **PerV$_{100}$** percentage of vegetation coverage within 100 m radius buffer zone. Same below.
*p < 0.05(two-tail).
** p < 0.01 (two-tail).

Table 4
Average PCII and PWII with standard deviation of 10 urban parks in Beijing.

	Summer noon	Summer night
PCII (℃)	1.09 ± 0.82	1.48 ± 0.92
Range (℃)	2.43	2.87
PWII (%)	3.63 ± 1.06	4.25 ± 5.63
Range (%)	3.04	17.89

composition factors are shown in Table 5. PS is the only correlated factor with nighttime PCII and PWII, while no significant correlation is found for daytime. Fig. 5 shows the relation between PCII, PWII and PS. Significant linear models were established for nighttime PCII and PWII (Fig. 5(c), (d)). For every 100 ha increase in PS, PCII shall increase 0.90℃, and PWII shall increase 3.98 %. However, due to the limited number of park samples, no threshold of PS could be identified.

4. Discussion

4.1. Quantification of atmospheric PCII

Urban parks have long been proved as cool islands in cities, and the intensity have been widely studied (Akbari and Kolokotsa, 2016). In this research, PCII of 10 large urban parks in Beijing ranges 0.11–3.22 ℃ in summer, which is similar to past observations in multiple cities across the world (Bowler et al., 2010).

However, great difficulties exist when comparing observed PCII among different studies, for the method used for the quantification of PCII in previous research varies in multiple ways. One dominant difference is the condition of the selected sampling points. Although most studies had selected unshaded sampling points out of urban parks (Chang et al., 2007; Monteiro et al., 2016; Doick et al., 2014, Sugawara et al., 2021), the condition of sampling points within parks differs. Chang et al. (2007) and Chang and Li (2014) selected unshaded paved area at the center of each park, while Monteiro et al. (2016) and Doick et al. (2014) mounted data loggers under tree canopy. Cohen et al. (2012), Hwang et al. (2015) and Sugawara et al. (2021) selected points both under and without tree canopy.

Tree canopy may significantly influence the calculated PCII. Trees may cool the air through shading and evapotranspiration during daytime (Taha et al., 1991), with shading playing the dominant role (Manickathan et al., 2018). Daytime Ta variance in an urban park may be as high as 4 ℃ between shaded and unshaded sites (Yan and Dong, 2015). While at night, tree canopy may hamper the loss of heat and exhibit a warming effect (Taha et al., 1991). Therefore, stronger PCII during daytime while weaker PCII during nighttime may be obtained when Ta is measured solely under tree canopy in urban parks. This may give explanation to some previous controversies, such as different diurnal and nocturnal PCII characteristic (Sugawara et al., 2021; Doick et al., 2014), and the nonapparent relation between PCII and climatic region (Saaroni et al., 2018).

In this study, all sampling points were set on nonshaded paved area to avoid the dramatic influence from trees shading. Nighttime PCII of 10 selected urban parks were generally stronger than noontime (Table 4), which is consistent with the observations of Doick et al. (2014) and Yan et al. (2018) in London and Beijing, two temperate cities. Such diurnal
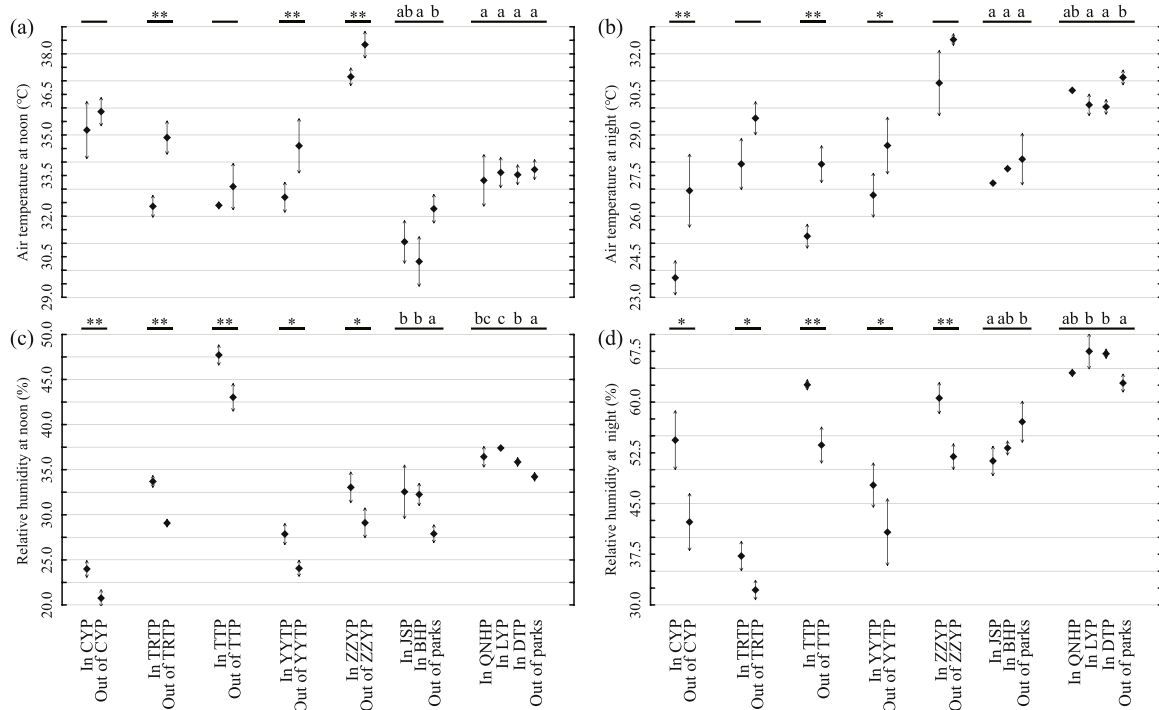
Fig. 4. Comparison of air temperature and relative humidity in and out of parks at noon ((a), (c)) and night ((b),(d)) in summer (For CYP, TYTP, TTP, YYTP and ZZYP, * refers to significant difference at α = 0.05, and ** refers to significant difference at α = 0.01. For JSP, BHP, QNHP, LYP, DTP, groups with identical letters are not significantly different at α = 0.05.).

Table 5
Correlation coefficients between PCII, PWII and influencing factors.

	PS	LSI	PerW	PerV	PerI
PCII at noon	−0.02	0.34	0.51	−0.50	−0.38
PWII at noon	0.18	−0.26	0.16	−0.13	−0.16
PCII at night	**0.88****	−0.06	−0.28	0.22	0.31
PWII at night	**0.64***	0.33	−0.08	0.13	−0.03

* $p < 0.05$ (two-tail).
** $p < 0.01$ (two-tail).

and nocturnal PCII difference complies with that of atmospheric heat island intensity of a city. In Beijing, urban heat island intensity is stronger at night than during daytime (Gao et al., 2019). One explanation is that the thermal properties of urban parks resemble that of rural areas and cools down more rapidly than urban area, and therefore lead to stronger difference at night (Deilami et al., 2018). However, such diurnal and nocturnal PCII difference seems to be climate sensitive, for Chang et al. (2007) recorded stronger noontime PCII in Taipei, a tropical city.

Another difference in previous studies is the reference used for the calculation of PCII. A commonly used reference point is at one-park width away from the park (Chang et al., 2007; Jaganmohan et al., 2016), which was based on the result of Jauregui (1990). While Jauregui (1990); Monteiro et al. (2016), etc., had selected fixed monitoring sites as reference, either in urban or rural area. In this research, like Yan et al. (2018), the average Ta of samples along a fixed traverse was used as the reference, so that the results of the two research could be compared. PCII of the 680 ha Beijing Olympic Forest Park, the largest urban park in core Beijing, was quantified as 2.8℃ at night in summer (Yan et al., 2018). Comparatively, PCII of 285 ha CYP and 198 ha TTP in this research are 3.22℃ and 2.66℃ respectively. Such results may serve as implications of the strongest PCII in Beijing, for there are no other larger urban parks located in heavily constructed urbanized area in Beijing. This also reflects a bottleneck of empirical studies of PCII that there are very few

large parks, making the statistic models less reliable as PS becomes larger and bringing difficulties to finding the key thresholds.

Additionally, in this research, by using polynomial regression, more effective cooling effects of an urban park were identified within approximately one-park width. This might support using the reference point at one-park width for the quantification of PCII, even though as Bowler et al. (2010) had pointed out, PCII in previous studies are unavoidably underestimated, for the cooling effect always extends beyond the selected reference point.

4.2. Large urban parks' local-scale climate effects

Urban parks may significantly influence their adjacent neighborhood (Jaganmohan et al., 2016; Monteiro et al., 2016). Significant Ta and Rh gradients were also observed in this research (Fig. 2). Such gradients were more significant at night than at noon (Fig. 2 and Table 2), for greater air mixing and more anthropogenic heat production lead to less stable thermal environment during daytime (Oke, 2006). For the same reason, stronger PCII and PWII were also observed at night (Table 4), though this doesn't necessarily mean weaker local-scale climate effect during daytime, for stronger breeze during daytime might better transfer cooler air to parks' surrounding area (Sugawara et al., 2021). How wind interacts with urban parks' local-scale climate effect deserves further investigations.

Urban parks' local-scale climate effect is influenced by multiple factors, among which PS plays the dominant role (Jaganmohan et al., 2016; Monteiro et al., 2016; Jauregui, 1990). Cooling effect of large urban parks in a city is considerable. Results of this research indicate that the cooling distance of 5 individual parks ranging 45.23–285.25 ha may reach 0.4−1 km (Fig. 2), smaller than the observed 1.4 km cooling distance of the 680 ha urban park in Beijing (Yan et al., 2018). Such results comply with the rule that larger parks have greater cooling distances, even though the relation between cooling distance and PS may not be as linear as conjectured by Monteiro et al. (2016).
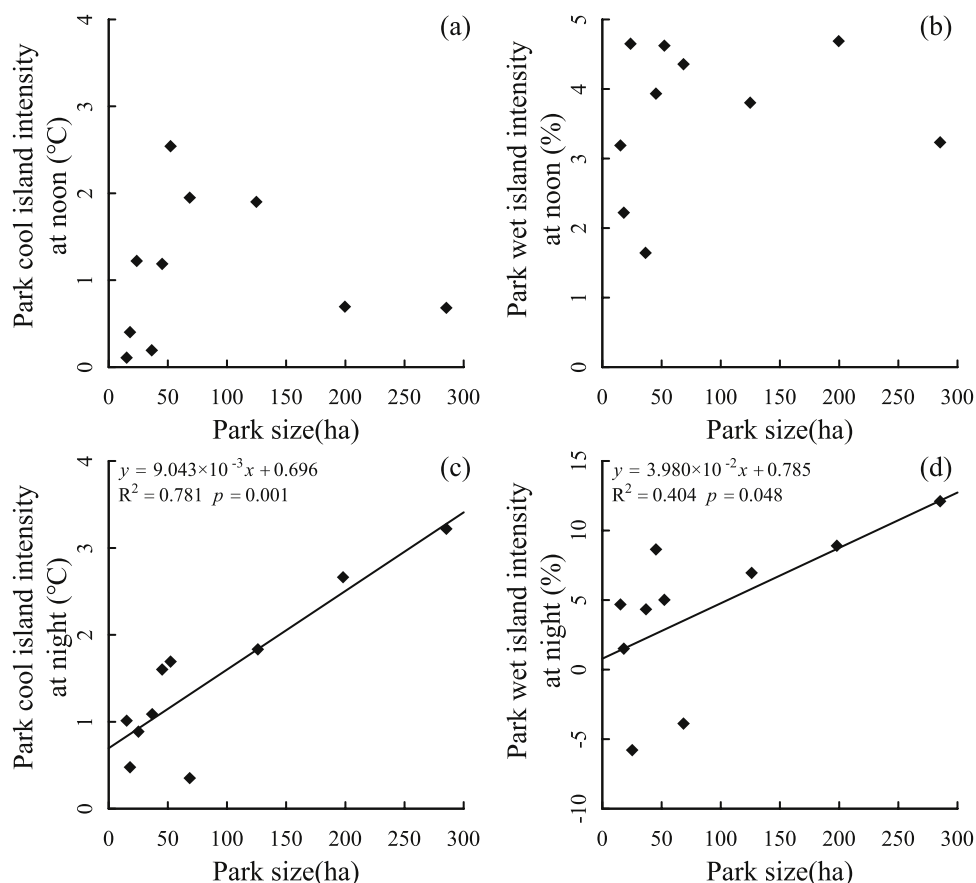
Fig. 5. Relation between park cool and wet island intensity and park size.

4.3. Potential insights for green spaces planning and design practice

Decades of study on PCII were aimed at providing guidance for urban green spaces planning and design. The size, shape and configuration of green spaces were paid the most attention, and are also the main influencing factors on PCII (Yu et al., 2020b).

PS, long been known as non-linearly correlated with PCII (Bowler et al., 2010), has been most widely discussed. Studies based on LST are inclined to believe that small parks, those generally smaller than 10 ha, are of higher efficiency for cooling the city (Fan et al., 2019; Yang et al., 2020; Yu et al., 2018). Empirical studies, though limited by the size of parks selected, also reached similar conclusions (Lu et al., 2012; Doick et al., 2014). Such threshold values are climate sensitive (Fan et al., 2019) and surely vary based on the research method used (Liao et al., 2021). While compared to smaller parks, our research strengthens that large parks are indispensable in regulating urban climate for their stronger cooling and humidifying intensity and further influencing distances. Even though more effective cooling might be obtained by constructing several small parks than an individual large one, compared to large parks, thermal environment in a small park is less stable due to significant edge effects (Jiao et al., 2017). Some small parks were even observed as heat islands in a city (Chang et al., 2007). Constructing large urban parks may better provide stable cool islands, and cast greater influence on adjacent areas.

Besides PS, another factor that may influence park's climate effect is its inner configuration. This research espouses the idea that high vegetation coverage guarantees a steady cooling effect. All selected sites in this research feature high vegetation coverage (Table 1), higher than the previously proposed 30 % threshold by Chang and Li (2014). This may also give explanation to why land cover composition was not found correlated with PCII or PWII in this research (Table 5). According to

Code for the Design of Public Park (MOHURD, 2016), urban parks in mainland China are required to have more than 65 % of its land (water body not included) covered by vegetation, which had effectively ensured steady cooling effects of urban parks.

Urban parks, as an important component of urban green-blue infrastructure, do not regulate urban climate alone but with other green-blue spaces, e.g., urban canals, street trees, pocket gardens, etc. (Hami et al., 2019; Taleghani, 2018). Better arrangement of green spaces in a city is expected to provide better regulation on urban climate. The multiple linear regression models built in this research were aimed at examining the climate effect interaction of large urban parks and their surrounding urban greenery. Results showed that even though PS of the selected parks was the dominant influencing factor on nighttime dTa and dRh (Table 3, $\beta = 0.64$, $\beta=-0.55$), RD and $PerV_{100}$ also had significant and strong impacts. $PerV_{100}$, which comprises of street trees, pocket gardens, community gardens, etc., quantifies the vegetation coverage around the sampling points out of urban parks, and were found contributing to decreasing the Ta and Rh difference between samples in an d out of parks, reflecting a positive impact on local-scale climate (Table 3, $\beta=-0.33$, $\beta = 0.36$). Such results indicate the significance of pedestrian level greenery, featuring small in size and scattered in arrangement, on cooling and humidifying the neighborhood. Similarly, Jaganmohan et al. (2016) also reported the positive influence of the greenery surrounding parks on extending parks' cooling distance and increasing cooling intensity. Studies implementing remotely sensed data had also pointed out the significance of land cover composition around urban parks on parks' cooling distance and intensity (Fan et al., 2019; Xu et al., 2017).

Therefore, based on results of this study, a green spaces planning scenario with large urban parks distributed according to their potential cooling distances surrounded by scattered pedestrian level greenery

could be proposed. Large urban parks may provide stable cooling and humidifying effects, while urban greenery may assist strengthening their cooling intensity and extending their cooling distances. Considering that effective cooling of large urban parks was detected within approximate one-park width by using polynomial regression models in this research (Fig. 3(c)), it may serve as an ideal distance between parks, though further investigation is needed either by including more smaller parks or by including similar investigation in other seasons.

Past simulation studies and research synthesis studies had led to some similar green spaces planning scenarios (Lin and Lin, 2016; Yu et al., 2020a,). Based on simulation results of a neighborhood, Lin and Lin (2016) had proposed one large park surrounded by several evenly distributed small neighborhood parks that could well regulate neighborhood thermal environment. Based on past research synthesis, Yu et al. (2020a) deduced a hierarchical hexagonal structure green spaces planning pattern with large green spaces surrounded by a mixture of smaller ones. The empirical evidence provided in this research may give urban planners and designers a better view of how urban green spaces, especially large urban parks may contribute to building a more thermally friendly city.

5. Conclusion

In this research, large urban parks' influence on summertime local-scale climate as well as park atmospheric cool and wet island intensity and their influencing factors were quantified and analyzed by field measurement in and around 10 parks in Beijing, China. Some parks were found significantly cooler or wetter than their surrounding urban area. Parks' influence on local-scale climate were significant, which had extended as far as over 1 km. Effective cooling and humidifying during summer nights were detected within the distance of approximately one-park width. Among all parameters, park size plays dominant role in influencing park cool and wet island intensity and parks' local-scale climate effect, with larger parks demonstrating stronger climate-regulating ability. Besides the impacts of urban parks, pedestrian level greenery also contributed significantly to regulating local-scale climate. Given the knowledge of this research, urban planners and designers should give priority to the layout of small and scattered urban greenery surrounding large urban parks distributed based on their cooling / humidifying distances. Such local-scale climate regulating distances are still awaiting further study, by either using multiple research methods or selecting a wider range of climate zones across the world.

Author statement

Yilun Li: Conceptualization, Methodology, Formal analysis, Investigation, Writing-Original Draft
Shuxin Fan: Methodology, Writing-Reviewing and Editing
Kun Li: Writing-Reviewing and Editing
Yue Zhang: Investigation
Lingxu Kong: Investigation
Yafen Xie: Investigation
Li Dong: Resources, Supervision, Project administration, Funding acquisition, Writing-Reviewing and Editing

Declaration of Competing Interest

The authors report no declarations of interest.

Appendix A. Background meteorology condition during data sampling

Study site(s)	Sampling date	Sampling time	Background meteorology condition						
			Ta(℃)	Rh(%)	v (m/s)	WD (°)	PM_{10} (µg/m$_3$)	$PM_{2.5}$ (µg/m$_3$)	AQI
CYP	Aug. 27, 2019	13:10-14:15	35.98	19.85	1.6[#]	261[#]	8 [A]	2 [A]	33 [A]
	Aug. 22, 2019	20:40-21:25	27.30	39.03	0.9[#]	12[#]	55 [A]	18[A]	53 [A]
TTP	Aug. 19, 2019	13:10-14:00	33.35	41.80	1.8[#]	160[#]	65 [B]	44 [B]	95 [B]
	Aug. 18, 2019	20:40-21:20	28.35	49.83	0.4[#]	101[#]	71 [B]	14[B]	61 [B]
YYTP	Aug. 23, 2019	13:00-14:00	32.80	25.00	0.7[#]	261[#]	21 [C]	13 [C]	35 [C]
	Aug. 21, 2019	20:25-21:05	29.08	35.95	0.4[*]	76[*]	31 [C]	19 [C]	31 [C]
TRTP	Aug. 24, 2019	13:20-14:10	33.83	30.08	1.6[#]	159[#]	34 [B]	18 [B]	79 [B]
	Aug. 27, 2019	20:30-21:15	29.83	31.45	1.4[#]	275[#]	19 [B]	8 [B]	25 [B]
ZZYP	Jul. 31, 2019	13:00-13:45	37.43	29.18	1.1[*]	208[*]	18 [C]	12 [C]	87 [C]
	Jul. 31, 2019	21:10-21:45	32.53	49.63	1.0[*]	18[*]	48 [C]	21[C]	77 [C]
LYP, QNHP, DTP	Aug. 14, 2019	13:20-14:40	33.75	33.95	0.5[*]	286[*]	N/A [D]	8 [D]	33 [D]
	Aug. 8, 2019	20:25-21:35	31.08	61.45	1.8[#]	164[#]	53 [D]	30[D]	52 [D]
JSP, BHP	Aug. 21, 2019	13:10-14:00	32.28	27.38	0.6[#]	265[#]	N/A [D]	11 [D]	37 [D]
	Aug. 14, 2019	20:20-21:10	29.00	51.75	0.9[#]	51[#]	42 [D]	12 [D]	42 [D]

v average wind speed within 2 min, **WD** average wind direction within 2 min, **PM_{10}**, **$PM_{2.5}$** concentration of particulate matter, **AQI** air quality index.

Data source: **Ta** and **Rh** were filed measured data at the reference point at the beginning of each sampling process. The rest were collected from local meteorology or air quality monitoring stations measured at 14:00 or 21:00 for daytime and nighttime respectively. v and **WD** were collected from the closest meteorology station with available data. Data marked with [#] from Chaoyang Station (54433), [*] from Haidian Station (54399). **PM_{10}**, **$PM_{2.5}$** and **AQI** were collected from local air quality monitoring station. Data marked with [A] from Nongzhanguan Station (110000247), [B] from Tiantan Station (110000245), [C] from Guanyuan Station (110000250), [D] from Dongsi Station (110000244).

References

Akbari, H., Kolokotsa, D., 2016. Three decades of urban heat islands and mitigation technologies research. Energy Build. 133, 834–842.

Allen, M.R., Dube, O.P., Solecki, W., et al., 2018. Framing and context. In: Masson-Delmotte, V., Zhai, P., Pörtner, H.O. (Eds.), Global Warming of 1.5°C., pp. 51–53. In press.

Altunkasa, C., Uslu, C., 2020. Use of outdoor microclimate simulation maps for a planting design to improve thermal comfort. Sustain. Cities Soc. 57, 102137.

Barradas, V.L., 1991. Air temperature and humidity and human comfort index of some city parks of Mexico city. Int. J. Biometeorol. 35 (1), 24–28.

Bartesaghi Koc, C., Osmond, P., Peters, A., 2018. Evaluating the cooling effects of green infrastructure: a systematic review of methods, indicators and data sources. Sol. Energy 166, 486–508.

Bowler, D.E., Buyung-Ali, L., Knight, T.M., Pullin, A.S., 2010. Urban greening to cool towns and cities: a systematic review of the empirical evidence. Landsc. Urban Plan. 97 (3), 147–155.

Chang, C., Li, M., 2014. Effects of urban parks on the local urban thermal environment. Urban For. Urban Green. 13 (4), 672–681.

Chang, C., Li, M., Chang, S., 2007. A preliminary study on the local cool-island intensity of Taipei city parks. Landsc. Urban Plan. 80 (4), 386–395.

Cohen, P., Potchter, O., Matzarakis, A., 2012. Daily and seasonal climatic conditions of green urban open spaces in the Mediterranean climate and their impact on human comfort. Build. Environ. 51, 285–295.

Coseo, P., Larsen, L., 2014. How factors of land use/land cover, building configuration, and adjacent heat sources and sinks explain Urban Heat Islands in Chicago. Landsc. Urban Plan. 125, 117–129.

Deilami, K., Kamruzzaman, M., Liu, Y., 2018. Urban heat island effect: a systematic review of spatio-temporal factors, data, methods, and mitigation measures. Int. J. Appl. Earth Obs. Geoinf. 67, 30–42.

Doick, K.J., Peace, A., Hutchings, T.R., 2014. The role of one large greenspace in mitigating London's nocturnal urban heat island. Sci. Total Environ. 493, 662–671.

Dorigon, L.P., Amorim, M.C.D.C., 2019. Spatial modeling of an urban Brazilian heat island in a tropical continental climate. Urban Clim. 28, 100461.

Epstein, Y., Moran, D.S., 2006. Thermal comfort and the heat stress indices. Ind. Health 44 (3), 388–398.

Fan, H., Yu, Z., Yang, G., Liu, T.Y., Liu, T.Y., Hung, C.H., Vejre, H., 2019. How to cool hot-humid (Asian) cities with urban trees? An optimal landscape size perspective. Agric. For. Meteorol. 265, 338–348.

Gao, Z., Hou, Y., Chen, W., 2019. Enhanced sensitivity of the urban heat island effect to summer temperatures induced by urban expansion. Environ. Res. Lett. 14 (9), 094005.

Hami, A., Abdi, B., Zarehaghi, D., Maulan, S.B., 2019. Assessing the thermal comfort effects of green spaces: a systematic review of methods, parameters, and plants' attributes. Sustain. Cities Soc. 49, 101634.

Harrell, F., 2018. Hmisc: Harrell miscellaneous. R Package Version 4.1-1.

Hothorn, T., Bretz, F., Westfall, P., 2008. Simultaneous inference in general parametric models. Biom. J. 50 (3), 346–363.

Huang, K., Li, X., Liu, X., Seto, K.C., 2019. Projecting global urban land expansion and heat island intensification through 2050. Environ. Res. Lett. 14 (11), 114037.

International Standard Organization, 1998. ISO 7726, Thermal environments: Instruments and Methods for Measuring Physical Quantities. ISO, Geneva.

Jaganmohan, M., Knapp, S., Buchmann, C.M., Schwarz, N., 2016. The bigger, the better? The influence of urban green space design on cooling effects for residential areas. J. Environ. Qual. 45 (1), 134–145.

Jauregui, E., 1990. Influence of a large urban park on temperature and convective precipitation in a tropical city. Energy Build. 15 (3), 457–463.

Jiao, M., Zhou, W., Zheng, Z., Wang, J., Qian, Y., 2017. Patch size of trees affects its cooling effectiveness: a perspective from shading and transpiration processes. Agric. For. Meteorol. 247, 293–299.

Kovats, R.S., Hajat, S., 2008. Heat stress and public health: a critical review. Annu. Rev. Public Health 29 (1), 41–55.

Li, Y., Fan, S., Li, K., Zhang, Y., Dong, L., 2021. Microclimate in an urban park and its influencing factors: a case study of Tiantan Park in Beijing, China. Urban Ecosyst. 24 (4), 767–778.

Liao, W., Cai, Z., Feng, Y., Gan, D., Li, X., 2021. A simple and easy method to quantify the cool island intensity of urban greenspace. Urban For. Urban Green., 127173

Lin, B., Lin, C., 2016. Preliminary study of the influence of the spatial arrangement of urban parks on local temperature reduction. Urban For. Urban Green. 20, 348–357.

Lin, P., Lau, S.S.Y., Qin, H., Gou, Z., 2017. Effects of urban planning indicators on urban heat island: a case study of pocket parks in high-rise high-density environment. Landsc. Urban Plan. 168, 48–60.

Lu, J., Li, C., Yang, Y., Zhang, X., Jin, M., 2012. Quantitative evaluation of urban park cool island factors in mountain city. J. Cent. South Univ. 19 (6), 1657–1662.

Manickathan, L., Defraeye, T., Allegrini, J., Derome, D., Carmeliet, J., 2018. Parametric study of the influence of environmental factors and tree properties on the transpirative cooling effect of trees. Agric. For. Meteorol. 248, 259–274.

Masoudi, M., Tan, P.Y., 2019. Multi-year comparison of the effects of spatial pattern of urban green spaces on urban land surface temperature. Landsc. Urban Plan. 184, 44–58.

Ministry of Housing and Urban-Rural Development of PRC, 2016. Code for the Design of Public Park (GB 51192-2016). China Architecture & Building Press, China. In Chinese.

Monteiro, M.V., Doick, K.J., Handley, P., Peace, A., 2016. The impact of greenspace size on the extent of local nocturnal air temperature cooling in London. Urban For. Urban Green. 16, 160–169.

National Bureau of Statistics of China (Beijing), 2020. Beijing Statistical Yearbook 2019. China Statistics Press, Beijing.

Oke, T.R., 1992. Boundary Layer Climates (Second Edition). Routledge, London, New York.

Oke, T.R., 1995. The heat Island of the urban boundary layer: characteristics, causes and effects. In: Cermak, J.E., Davenport, A.G., Plate, E.J., Viegas, D.X. (Eds.), Wind Climate in Cities. NATO ASI Series (Series E: Applied Sciences), vol 277. Springer, Dordrecht.

Oke, T.R., 2006. Initial guidance to obtain representative meteorological observations at urban sites. WMO Report 1–47.

Oke, T.R., Mills, G., Christen, A., Voogt, J.A., 2017. Urban Climates. Cambridge University Press, UK.

Peng, J., Xie, P., Liu, Y., Ma, J., 2016. Urban thermal environment dynamics and associated landscape pattern factors: a case study in the Beijing metropolitan region. Remote Sens. Environ. 173, 145–155.

R Development Core Team, 2015. R: a Language and Environment for Statistical Computing.

Saaroni, H., Amorim, J.H., Hiemstra, J.A., Pearlmutter, D., 2018. Urban Green Infrastructure as a tool for urban heat mitigation: survey of research methodologies and findings across different climatic regions. Urban Clim. 24, 94–110.

Shashua-Bar, L., Hoffman, M.E., 2000. Vegetation as a climatic component in the design of an urban street: an empirical model for predicting the cooling effect of urban green areas with trees. Energy Build. 31 (3), 221–235.

Sodoudi, S., Zhang, H., Chi, X., Müller, F., Li, H., 2018. The influence of spatial configuration of green areas on microclimate and thermal comfort. Urban For. Urban Green. 34, 85–96.

Sugawara, H., Narita, K., Mikami, T., 2021. Vertical structure of the cool island in a large urban park. Urban Clim. 35, 100744.

Taha, H., Akbari, H., Rosenfeld, A., 1991. Heat island and oasis effects of vegetative canopies: micro-meteorological field-measurements. Theor. Appl. Climatol. 44 (2), 123–138.

Taleghani, M., 2018. Outdoor thermal comfort by different heat mitigation strategies – a review. Renew. Sustain. Energy Rev. 81, 2011–2018.

Xu, X., Cai, H., Qiao, Z., Wang, L., Jin, C., Ge, Y., Wang, L., Xu, F., 2017. Impacts of park landscape structure on thermal environment using QuickBird and Landsat images. Chin. Geogr. Sci. 27 (5), 818–826.

Yan, H., Dong, L., 2015. The impacts of land cover types on urban outdoor thermal environment: the case of Beijing, China. J. Environ. Health Sci. Eng. 13 (1).

Yan, H., Fan, S., Guo, C., Hu, J., Dong, L., 2014a. Quantifying the impact of land cover composition on intra-urban air temperature variations at a mid-latitude city. PLoS One 9 (7), e102124.

Yan, H., Fan, S., Guo, C., Wu, F., Zhang, N., Dong, L., 2014b. Assessing the effects of landscape design parameters on intra-urban air temperature variability: the case of Beijing, China. Build. Environ. 76, 44–53.

Yan, H., Wu, F., Dong, L., 2018. Influence of a large urban park on the local urban thermal environment. Sci. Total Environ. 622-623, 882–891.

Yang, C., He, X., Yu, L., Yang, J., Yan, F., Bu, K., Chang, L., Zhang, S., 2017. The cooling effect of urban parks and its monthly variations in a snow climate city. Remote Sens. 9 (10), 1066.

Yang, G., Yu, Z., Jørgensen, G., Vejre, H., 2020. How can urban blue-green space be planned for climate adaption in high-latitude cities? A seasonal perspective. Sustain. Cities Soc. 53, 101932.

Yu, Z., Guo, X., Jørgensen, G., Vejre, H., 2017. How can urban green spaces be planned for climate adaptation in subtropical cities? Ecol. Indic. 82, 152–162.

Yu, Z., Guo, X., Zeng, Y., Koga, M., Vejre, H., 2018. Variations in land surface temperature and cooling efficiency of green space in rapid urbanization: the case of Fuzhou city, China. Urban For. Urban Green. 29, 113–121.

Yu, Z., Fryd, O., Sun, R., Jørgensen, G., Yang, G., Özdil, N.C., Vejre, H., 2020a. Where and how to cool? An idealized urban thermal security pattern model. Landsc. Ecol.

Yu, Z., Yang, G., Zuo, S., Jørgensen, G., Koga, M., Vejre, H., 2020b. Critical review on the cooling effect of urban blue-green space: a threshold-size perspective. Urban For. Urban Green. 49, 126630.